J Solid State Electrochem (2001) 5: 512–521
DOI 10.1007/s100080100195

ORIGINAL PAPER

Yulia V. Basova

Preparation and electrochemical properties of catalysts based on macrobicyclic d-metal tris-dioximate complexes

Received: 3 September 2000 / Accepted: 22 December 2000 / Published online: 3 July 2001

Abstract The use of macrobicyclic tris-dioximate complexes of cobalt, $K_3[Co(Dmg)_3]$ (where $DmgH_2 = C_4H_8N_2O_2$), and iron, $(BPh)_2[Fe(Nx)_3]$ (where $NxH_2 = C_6H_{10}N_2O_2$), and the carbon-supported complexes and their pyrolyzates, as catalysts for oxygen reduction was examined utilizing the combination of thermogravimetry, infrared spectroscopy, mass spectrometry and electrochemical techniques. The results have shown that macrobicyclic cobalt complexes adsorbed on the surface of carbon- based synthetic porous polymers have a pronounced catalytic effect on the reduction of molecular oxygen. A reduction in the oxygen overpotential was observed with heat treatment of the catalysts prepared in an inert atmosphere. The optimum pyrolysis temperature for the electrochemically most active catalysts for oxygen reduction was estimated.

Keywords Synthetic carbon · Macrobicyclic complex · Electrochemical properties · Catalysts

Introduction

The search for effective and relatively inexpensive catalysts for electroreduction of molecular oxygen has been heightened in many research studies because of the increasing technological importance of energy conversion/storage systems used in fuel cell and air batteries. Sufficient evidence for the effective performance of an oxygen electrode achieved by use of various porphyrin or phthalocyanine compounds [1, 2, 3, 4, 5, 6, 7, 8, 9, 10], or these compounds attached to the surface of carbon materials followed by thermal treatment in an inert atmosphere, has been presented [11, 12, 13, 14, 15]. Most recently, macrobicyclic tris-dioximate complexes, in which the transition metal ion is coordinatively saturated and surrounded by ligands, have been described as promising oxidation-reduction catalysts and electron carriers [16, 17, 18, 19]. Such macrobicyclic complexes have an ability to catalyze electrochemical reactions, including oxygen reduction in aqueous media, and can be utilized over a wide pH range that appears advantageous for the catalysts and electrode preparation. On the other hand, carbon materials prepared from synthetic co-polymers and resins are advantageous support materials, owing to their unique physicochemical properties [17, 18, 19], for the preparation of high-performance catalysts through their surface modification.

The object of this work is to develop a novel catalytic material that would be easy to produce and highly effective in electrocatalytic reactions. The interest in the enhancing of electrocatalytic reactions involving molecular oxygen has prompted the examination of the electrochemical behavior of the macrobicyclic complexes of cobalt and iron and their catalyst/electrode combinations with synthetic carbon supports before and after subjecting them to various thermal treatments.

Presented at the international conference "Solid State Chemistry 2000", 3–8 September 2000, Prague, Czech Republic

Y.V. Basova (✉)
National Institute of Advanced Industrial Science and Technology, 2217-14 Hayashi-cho, Takamatsu-shi, Kagawa, 761-0395, Japan
E-mail: yulia.basova@aist.ga.jp
Tel.: +81-87-8693511
Fax: +81-87-8693551

Y.V. Basova
Institute for Sorption and Problems of Endoecology, 13 General Naumov Str., Kiev, Ukraine

Experimental

Specimen preparation

The investigation covered two types of spherically granulated synthetic carbons used as the carbon support, obtained by carbonization and activation of (1) co-polymers of styrene with divinylbenzene (SCS) and (2) co-polymers of vinylpyridine with divinylbenzene (SCN) (BET surface area 880 m^2/g and 1320 m^2/g, respectively). The macrobicyclic tris-dioximate complexes $K_3[Co(Dmg)_3]$ (where $DmgH_2 = C_4H_8N_2O_2$) [20] and $(BPh)_2[Fe(Nx)_3]$

(where $NxH_2 = C_6H_{10}N_2O_2$) [21], shown schematically in Fig. 1, were used for modification of the carbon surface.

The modification was performed by irreversible adsorption of the complexes on the surface of the carbon support. The adsorption of the complexes (up to 4 wt%) on the synthetic carbon surfaces was performed from 10^{-3} mol dm^{-3} $K_3[Co(Dmg)_3]$ in 50% aqueous acetonitrile solution and 10^{-3} mol dm^{-3} $(BPh)_2[Fe(Nx)_3]$ in acetonitrile solution for 24 h. The prepared materials were washed thoroughly in their respective solvents and dried at a temperature below 80 °C.

Chemical and physical surface characterization

To achieve possible structural changes, the specimens were subjected to thermogravimetric (TG-DTA) experiments. The experiments were performed in an argon atmosphere in a TG-DTA system (TAS-200 Rigaku, Japan) at a heating rate of 6°C min^{-1}. Phase transformations were identified in the temperature range 25–1000 °C. Hard pyrolytic products were analyzed by IR reflection spectroscopy in a spectrophotometer (JEOL 100 FTIR, Japan) in the range 2000–400 cm^{-1}. Volatile pyrolytic products were examined by electron flash mass spectrometry in a mass spectrometer (MH-1310, Russia). While the specimens (0.5 mg each) were heated in the range 20–1000 °C at a heating rate of 6°C min^{-1}, full mass spectra in the range 12–400 a.e.m. were continually recorded for every 20 °C increment in the temperature. Apparent surface areas and pore volumes of the carbon specimens were determined from physical adsorption measurements with N_2 at 77 K using a BELSORP 28SA (Japan) instrument.

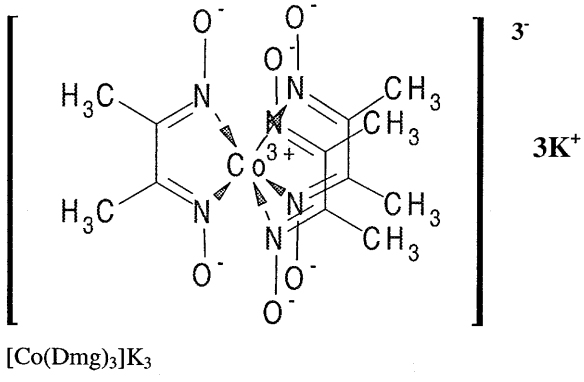

$[Co(Dmg)_3]K_3$

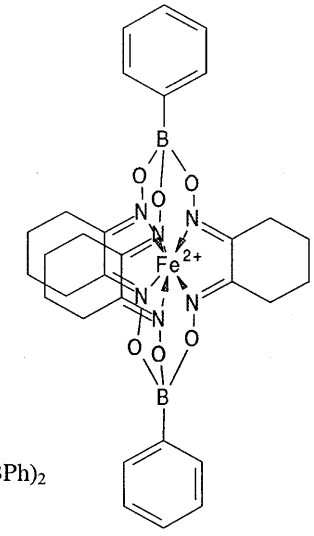

$[Fe(Nx)_3](BPh)_2$

Fig. 1 Macrobicyclic tris-dioximate complexes used in this study

Electrochemical measurements

The cyclic voltammetry measurements (CV) were performed with a typical set-up: a potentiostat and a functional generator with a three-electrode electrochemical cell. In this cell a non-porous carbon sphere, 1 mm in diameter, or a thin layer of the heat-treated complex powder attached to carbon conductive adhesive, were used as the working electrode. A Pt mesh was used as a counter electrode. All cyclovoltammetric experiments were performed with a functional generator (HB-105, Hokuto Denko, Japan) connected with a potentiostat (HA 501G, Hokuto Denko). The CV curves were recorded at 5–100 mV s^{-1} of the potential scan rate. The supporting electrolyte was 0.15 mol dm^{-3} NaCl. Helium gas (99.995%) was used for deaeration of the solution.

The steady potential versus pH (E_R-pH) diagrams were measured using the electrochemical cell with the fluidized-bed carbon layer described elsewhere [22]. The electrode potentials were measured and quoted versus a saturated Ag/AgCl reference electrode.

Results

Thermal decomposition of the as-prepared and carbon-supported complexes

$K_3[Co(Dmg)_3]$ complex

Figure 2 shows the weight loss as a function of the heating temperature recorded for the $K_3[Co(Dmg)_3]$ complex. From the TG-DTA diagram, below 270 °C no decomposition occurs except for dehydration of the specimen, verified by the appearance in the mass spectrum of only low molecular weight impurities, i.e. water ($m/e = 18$), acetonitrile ($m/e = 41$) and CO_2 ($m/e = 44$). When the temperature is raised from 270 to 670 °C, a two-step decomposition of the macrobicyclic structure of the complex occurs. The decomposition is confirmed by a significant weight loss, the relevant peak on the DTA curve, and the appearance of an additional signal in the mass spectrum with $m/e = 98$, corresponding to a derivative originating from the dimethylglyoximate ligands of the macrobicyclic structure. Further increase in the temperature leads to a non-significant gradual

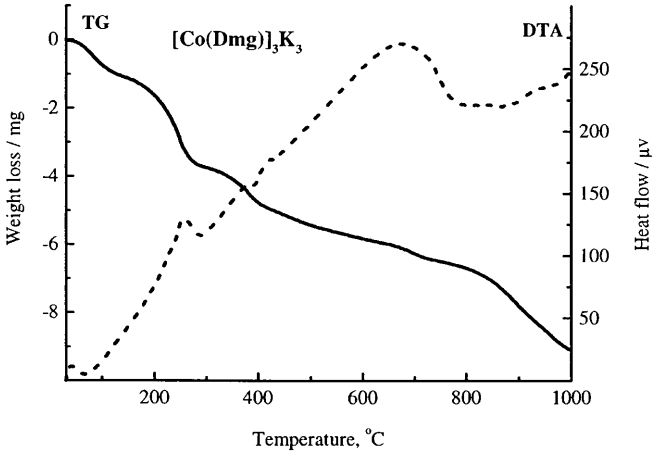

Fig. 2 Weight loss as a function of heating temperature for the $K_3[Co(Dmg)_3]$ complex

weight loss consistent with liberation of CO_2 ($m/e = 44$), CO ($m/e = 28$) and H_2 ($m/e = 2$).

Figure 3 displays the IR spectra of the $K_3[Co(Dmg)_3]$ complex, registered after each step of the decomposition. From Fig. 3, absorption bands associated with C=N stretching vibrations (1610 and 1535 cm^{-1}), N=O stretching vibrations (1215 and 1080 cm^{-1}) and $-CH_3$ bending vibrations (1440 and 1375 cm^{-1}) are registered before the thermal treatment. During the annealing process, in the temperature range 270–670 °C the absorption bands become wider and less intensive. Furthermore, the bands vanish when the temperature reaches 800 °C, and the spectrum becomes typical for elemental metal or carbon. Presumably, the increase of temperature (750–1000 °C) leads to the formation of pyropolymer compounds containing β-Co and carbon phases with various cobalt carbides, nitrides and oxides, also detected by X-ray diffraction patterns (DRON-UM1, Russia).

$(BPh)_2[Fe(Nx)_3]$ complex

Figure 4 shows the weight loss of the as-received $(BPh)_2[Fe(Nx)_3]$ complex. From the TG-DTA diagram, a significant weight loss of the $(BPh)_2[Fe(Nx)_3]$ complex is detected from 260 to 270 °C, accompanied by dehydration ($m/e = 18$) and release of furazane derivatives ($m/e = 98$). During the pyrolysis between 270 and 490 °C, additional lines corresponding to linked groups ($m/e = 102$–104), ligand fragments ($m/e = 124$) and products of side ring destruction ($m/e = 51$, 52, 83, 113) are detected. Presumably, thermodestruction of the complex proceeds through transformation to a flat macrocycle, which is accompanied by a significant weight loss and an exothermal effect. It is likely that the decomposition process is completed at 640–800 °C by the formation of pyropolymer compounds containing β-Fe.

The structural changes mentioned above are confirmed by analysis of the IR spectra of this complex, recorded after various heat treatments and shown in Fig. 5. Absorption bands associated with C=N stretching vibrations (1610 and 1535 cm^{-1}), N=O stretching vibrations (1215 and 1090 cm^{-1}) and B=O stretching vibration (1205 cm^{-1}) are detected for the as-prepared complex. With further heat treatment, the absorption bands become wider and less intensive, disappearing when the temperature exceeds 640 °C and thus confirming the presence of pyrolyzed products only.

Additionally, it should be noted that the transformation of the complexes adsorbed on the carbon supports showed the same tendency as for the pure compounds. However, separation of each destruction step is not well marked owing to the lower concentration of the complex on the carbon surface and the influence of the carbon support. The heat treatment of the materials does not produce significant changes in the textural properties of the prepared materials (Tables 1 and 2), making inaccessible only a small portion of the carbon pores.

Electrochemical measurements

$K_3[Co(Dmg)_3]$ complex

The electrochemical behavior of dissolved $K_3[Co(Dmg)_3]$ complex was examined on the SCS and SCN carbon electrodes in 0.15 mol dm^{-3} NaCl solution containing 10^{-3} mol dm^{-3} $K_3[Co(Dmg)_3]$. A typical set of cyclic voltammograms recorded at the SCS electrode

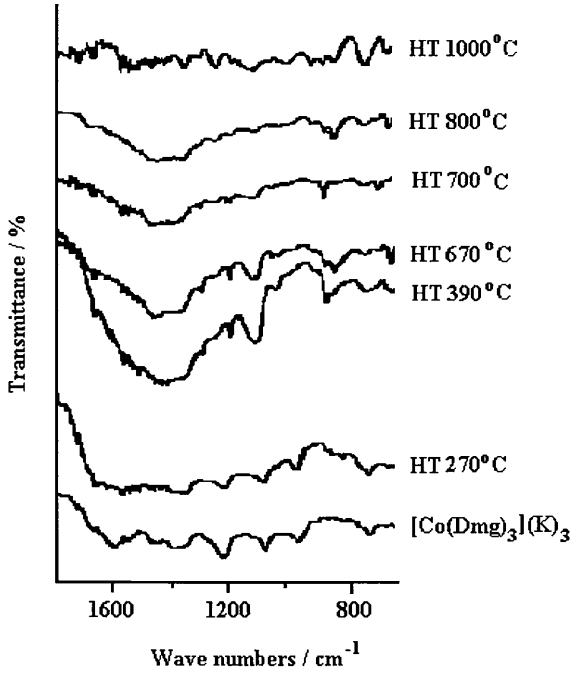

Fig. 3 IR spectra of the $K_3[Co(Dmg)_3]$ complex subjected to various heat treatments

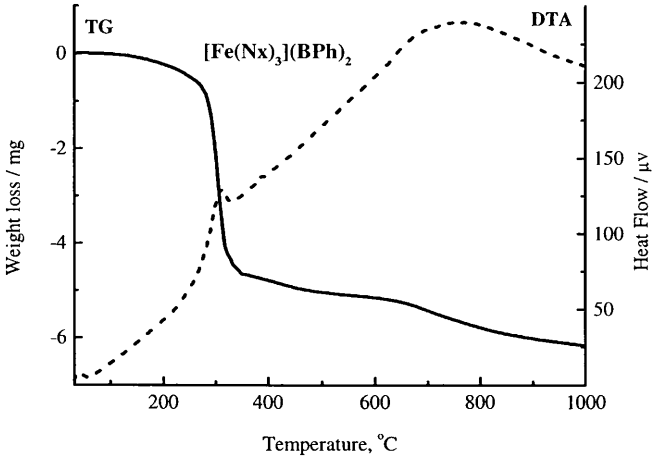

Fig. 4 Weight loss as a function of heating temperature for the $(BPh)_2[Fe(Nx)_3]$ complex

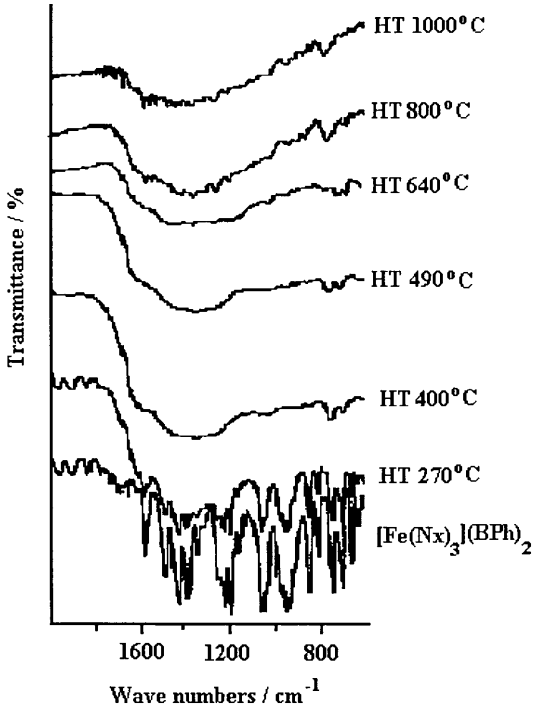

Fig. 5 IR spectra of the $(BPh)_2[Fe(Nx)_3]$ complex subjected to various heat treatments

are shown in Fig. 6. As seen in Fig. 6a, in the deaerated solution the $K_3[Co(Dmg)_3]$ complex gives rise to a pair of anodic, I^a_p, and cathodic, I^c_p, current peaks. Peak potential separation, $\Delta E = E^a_p - E^c_p$, is equal to 58 mV for the SCS and 70 mV for the SCN carbons, and the ratio I^a_p/I^c_p is equal to 1. When the carbon electrodes are immersed in oxygen-saturated 10^{-3} mol dm^{-3} $K_3[Co(Dmg)_3]$ solution, the current-potential response shows a pair of current peaks, for which $\Delta E = 80$ mV (SCS) and 150 mV (SCN) and with $I^a_p/I^c_p > 1$. Also, an additional peak appears at more negative potentials (ca. –0.35 to –0.4 V). A plot of this cathodic current peak, I^c_p, as a function of the square root of the electrode potential scan rate, $v^{1/2}$, is linear (Fig. 6b), indicating that the electrode reaction is controlled by diffusion of the reactant to the electrode surface.

The cyclic voltammograms recorded at the SCS-supported $K_3[Co(Dmg)_3]$ complex in the electrolyte solution devoid of the dissolved complex show a pair of current-potential peaks with $\Delta E = 57$ mV and $I^a_p/I^c_p = 1$ (Fig. 7a). The values of I^a_p and I^c_p were found to change linearly with an increase in the potential scan rate (Fig. 7b). The current peaks become less pronounced when the cyclic voltammograms are recorded on the SCN-supported $K_3[Co(Dmg)_3]$ complex electrode. The second electrochemical response is a diffusion-controlled cathodic wave, which commences at the cathodic potential range –0.6 to –0.75 V (Fig. 7a). It should be stressed that successive voltammetric scanning (100 cycles) produces no effect on the magnitude of the current peaks, indicating the durability of the adsorption of the complex on the carbon surface and the stability of the electrode performance.

The electrochemical behavior of both the as-prepared and carbon-supported $K_3[Co(Dmg)_3]$ complex electrodes was investigated as a function of the pyrolysis temperature. A summary of the CV measurements of the heat-treated $K_3[Co(Dmg)_3]$ complex is given in Fig. 8a. When the temperature is raised, the pair of current-potential peaks becomes less pronounced, whereas the limiting current of the second cathodic response increases slightly.

The cyclic voltammetric behavior of the carbon-supported complex follows the above tendency for the as-prepared complex except for a decrease in magnitude of the second cathodic response observed for the specimen heated to 670 °C (Fig. 8b).

Table 1 The textural properties of the as-prepared and heat-treated carbon-supported $K_3[Co(Dmg)_3]$ complex (N_2 adsorption at 77 K)

Specimen	SCS + $K_3[Co(Dmg)_3]$				SCN + $K_3[Co(Dmg)_3]$			
	As-prepared	Heat treatment (°C)			As-prepared	Heat treatment (°C)		
		390	670	800		390	670	800
Surface area, S_{BET} (m^2 g^{-1})	783	781	671	620	1115	1105	1087	1045
Micropore volume, V_m (cm^3 g^{-1})	158	156	148	135	289	282	247	242

Table 2 The textural properties of the as-prepared and heat-treated carbon-supported $(BPh)_2[Fe(Nx)_3]$ complex (N_2 adsorption at 77 K)

Specimen	SCS + $(BPh)_2[Fe(Nx)_3]$				SCN + $(BPh)_2[Fe(Nx)_3]$			
	As-prepared	Heat treatment (°C)			As-prepared	Heat treatment (°C)		
		490	640	800		490	640	800
Surface area, S_{BET} (m^2 g^{-1})	676	670	663	625	1098	1076	1034	1030
Micropore volume, V_m (cm^3 g^{-1})	145	140	135	128	252	248	237	236

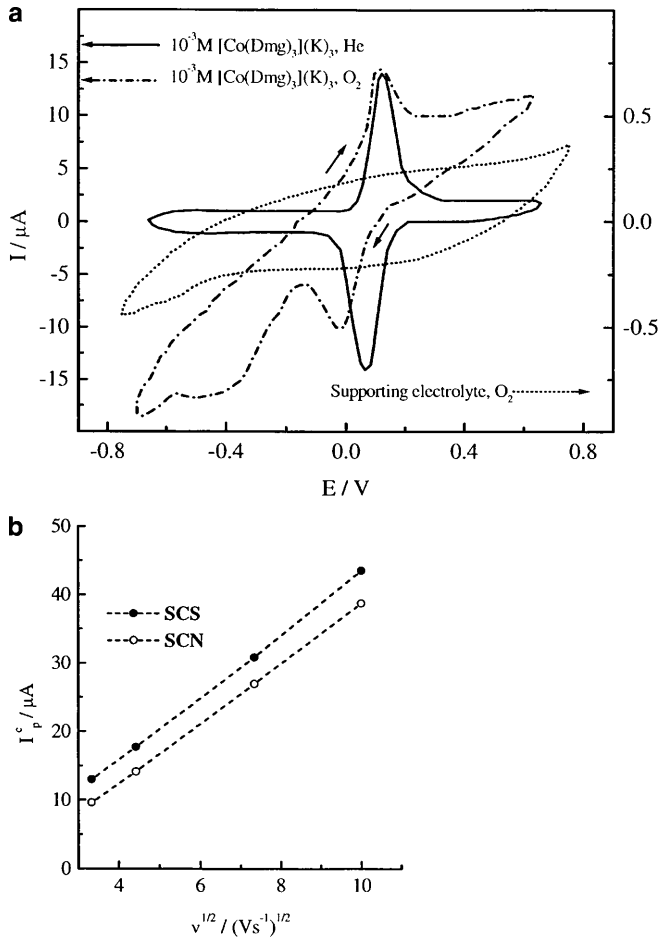

Fig. 6 **a** Cyclic voltammograms recorded at the SCS carbon electrode in 10^{-3} M $K_3[Co(Dmg)_3]$ solution in 0.15 mol dm^3 NaCl. Scan rate: 20 mV s^{-1}. **b** The value of the second cathodic peak limiting current, I^c_p, versus the square root of the potential scan rate, $v^{1/2}$, for the SCS and SCN carbon electrodes

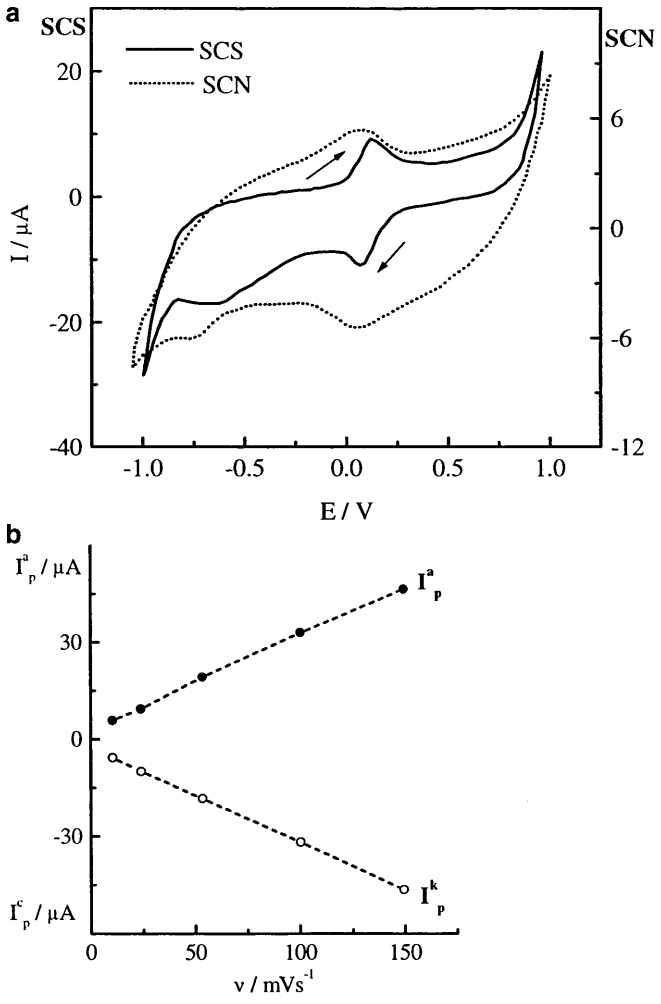

Fig. 7 **a** Cyclic voltammograms for the $K_3[Co(Dmg)_3]$ complex adsorbed on the SCS and SCN synthetic carbon supports. Scan rate: 20 mV s^{-1}; oxygen atmosphere. **b** The values of anodic peak, I^a_p, and cathodic peak, I^c_p, limiting currents versus the potential scan rate, v, recorded for the $K_3[Co(Dmg)_3]$ complex adsorbed on the SCS support

Figure 9 shows the E_R-pH diagrams measured for the carbon-supported complex treated at different temperatures. From the diagrams, the slope for both the SCS and SCN carbon supports increases when the $K_3[Co(Dmg)_3]$ complex is adsorbed on their surfaces. When the heating temperature is raised, the slope continues to increase, reaching its maximum at 800 °C, and it then becomes less when the temperature approaches 1000 °C.

Table 3 presents the estimates for the second cathodic peak and peroxide decomposition obtained from the CV measurements and investigations of the fluidized-bed electrode based on the above catalysts. It is seen in Table 3 that the adsorption of the $K_3[Co(Dmg)_3]$ complex on the surface of both carbon supports enhances significantly the decomposition of H_2O_2. The capability of decomposing H_2O_2 is evidently reduced when the specimen is treated in the interval 390–670 °C. Further heat treatment leads to almost entire decomposition of H_2O_2, followed by diminishing activity with further increase of the heating temperature.

$(BPh)_2[Fe(Nx)_3]$ complex

The electrochemistry of the $(BPh)_2[Fe(Nx)_3]$ complex was studied in acetonitrile and in 0.15 mol dm^{-3} NaCl solution. Figure 10 shows the cyclic voltammetric behavior of the as-prepared $(BPh)_2[Fe(Nx)_3]$ complex (Fig. 10a and b), and the complex subjected to heat treatment at various temperatures (Fig. 10b–d). Unlike the case of the $K_3[Co(Dmg)_3]$ complex, a well-resolved voltammetric response in the range of –0.5 to –0.57 V can be seen only for the specimen heat treated at 800–1000 °C. The cyclic voltammetric behavior of the carbon-supported $(BPh)_2[Fe(Nx)_3]$ complex was found to follow the same tendency as for the as-prepared complex. However, in the case of the SCS-supported $(BPh)_2[Fe(Nx)_3]$ complex, the voltammetric response was observed at a lower (640 °C) heating temperature.

From the E_R-pH diagrams, displayed in Fig. 11, the adsorption of the $(BPh)_2[Fe(Nx)_3]$ complex on the SCS

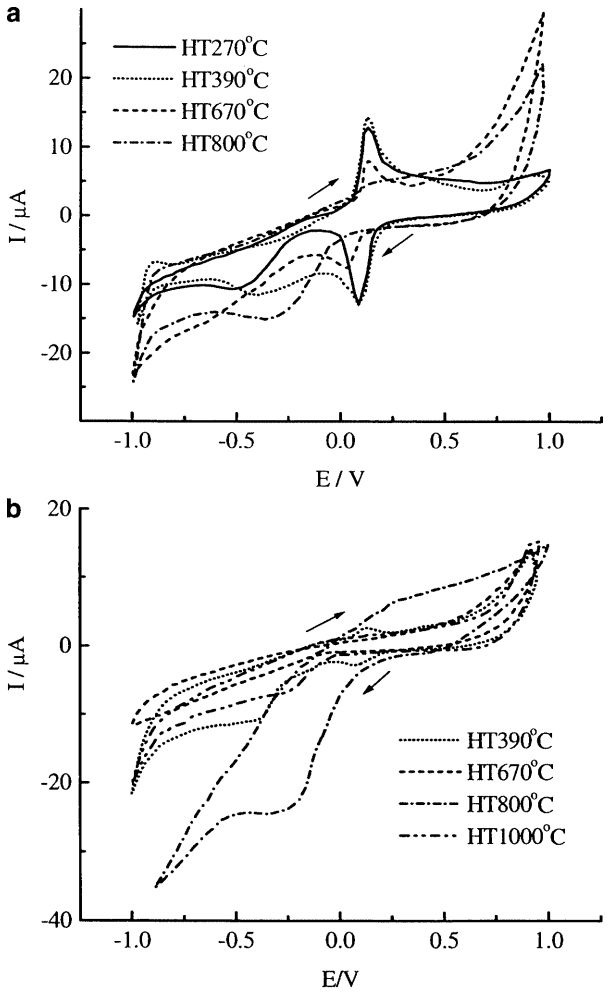

Fig. 8 **a** Cyclic voltammograms recorded for the $K_3[Co(Dmg)_3]$ complex heat treated at different temperatures. **b** Cyclic voltammograms recorded at the SCS-supported $K_3[Co(Dmg)_3]$ complex heat treated at different temperatures. Supporting electrolyte: 0.15 M NaCl; scan rate: 20 mV s^{-1}; oxygen atmosphere

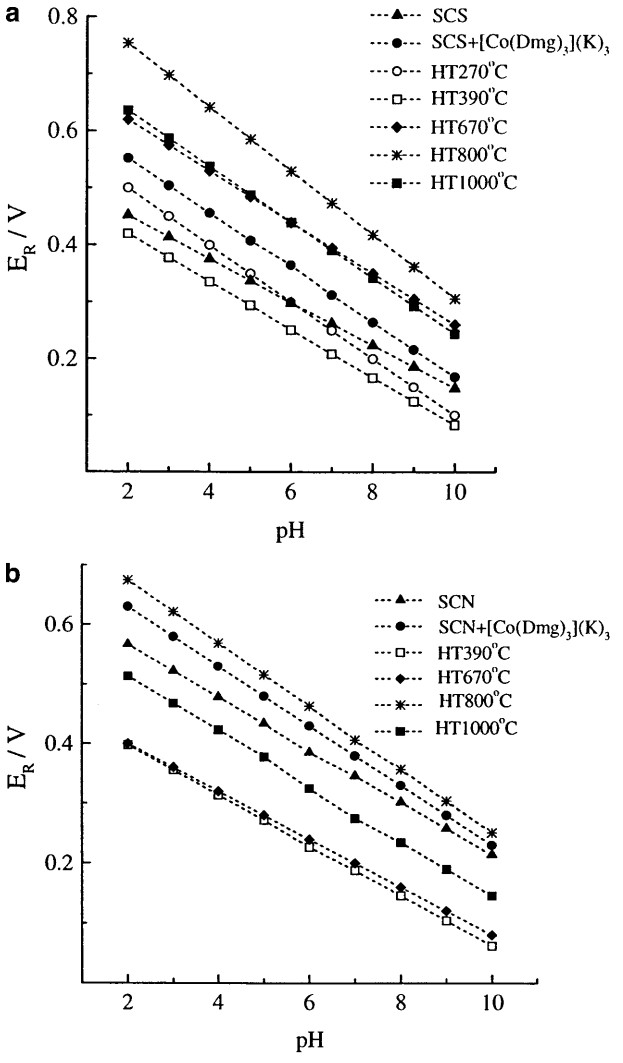

Fig. 9 The steady potential of the electrode, E_R, as a function of the pH for the **a** SCS- and **b** SCN-supported $K_3[Co(Dmg)_3]$ complex. Supporting electrolyte: 0.15 mol dm^{-3} NaCl; oxygen atmosphere

carbon support has no influence on the response of the E_R to the pH, although the response is slightly suppressed for the SCN carbon support. When the heating temperature is raised to 640 °C, the slope increases for the SCS carbon-supported complex and becomes maximal for both the SCS and SCN carbon-supported catalysts treated at 800–1000 °C. From Table 4, the SCS- and SCN-supported $(BPh)_2[Fe(Nx)_3]$ complexes demonstrate a similar tendency in catalytic activity in the peroxide decomposition reaction. The maximal rate of the decomposition is observed for both the catalysts treated at 800–1000 °C.

Discussion

From the electrochemical behavior of the $K_3[Co(Dmg)_3]$ complex and the prepared carbon-supported catalysts described above, two remarkable electrochemical responses can be seen. The nature of these electrochemical responses can be discussed on the basis of the results obtained from the measured cyclic voltammograms.

The first reversible voltammetric response, having $\Delta E = 58$–70 mV and $I^a_p/I^c_p = 1$, is attributable to a simple one-electron Nernstian Co^{3+}/Co^{2+} redox couple present in the solution of the dissolved complex. When adsorbed on the surface of the SCS carbon support, the $K_3[Co(Dmg)_3]$ complex becomes capable of a reversible voltammetric response, changing linearly with the scan rate, as was expected for the adsorbed reactants. It is noteworthy that the voltammetric peaks appear at potentials near those observed in the cyclic voltammograms recorded for this complex in the dissolved state (± 5 mV), suggesting good adsorption of the complex while the SCS carbon is immersed in the solution. Conversely, both peaks become broader for the SCN-supported complex, and the peak potential separation is approximately zero. These features reveal that the

Table 3 The variation in half-wave potential and hydrogen peroxide decomposition among the catalysts employed

Catalyst	$E_{1/2}$ (V)[a]	H_2O_2 decomposition (%)[b]	Specific rate of H_2O_2 decomposition (mol s^{-1} g^{-1})[c]
SCS	–0.56	15.6	0.27
SCS + K_3[Co(Dmg)$_3$]	–0.42	65.5	4.6
SCS + K_3[Co(Dmg)$_3$] (HT 390 °C)	–0.33	60.7	0.88
SCS + K_3[Co(Dmg)$_3$] (HT 670 °C)	–	26.1	0.67
SCS + K_3[Co(Dmg)$_3$] (HT 800 °C)	–0.08	100.0	9.5
SCS + K_3[Co(Dmg)$_3$] (HT 1000 °C)	–0.148	85.0	3.4
SCN	–0.70	27.3	0.65
SCN + K_3[Co(Dmg)$_3$]	–0.66	63.3	4.15
SCN + K_3[Co(Dmg)$_3$] (HT 390 °C)	–0.25	50.6	1.25
SCN + K_3[Co(Dmg)$_3$] (HT 670 °C)	–0.59	22.5	0.97
SCN + K_3[Co(Dmg)$_3$] (HT 800 °C)	–0.2	90.0	8.0
SCN + K_3[Co(Dmg)$_3$] (HT 1000 °C)	–0.4	57.8	2.3

[a]The potential at which the current of the second cathodic peak reaches one-half the limiting value
[b]Measured after 2 h of contact with the fluidized-bed layer of the catalyst
[c]Calculated for the first 30 min of the reaction

carbon support can adsorb the macrobicyclic complex, which probably takes place at different environmental sites on the SCS and SCN surfaces, as has also been reported elsewhere [23, 24].

With the CVs run in the oxygen-saturated electrolyte, the second diffusion-controlled cathodic response appears at more negative potentials, which is assumed to arise from the electroreduction of oxygen catalyzed by the presence of the complex in the solution. Actually, in the absence of the dissolved complex in the oxygen-saturated supporting electrolyte, a weak cathodic response can be discerned, whereas in the presence of the complex, a clearly resolved response occurs at more positive potentials. Taking into account the diffusion-controlled character of the second cathodic peak observed and the disappearance of the response in the oxygen-free solution, the catalytic effect on the oxygen electroreduction can be proved. The well-reproducible cathodic response of the oxygen reduction detected for the carbon-supported complex coincides with that detected for the dissolved complex, suggesting it has good performance as a catalyst when attached to the surface of the carbon support.

From the CV measurements of the as-prepared K_3[Co(Dmg)$_3$] complex and the carbon-supported complex in the temperature range studied, the incremental change in the heating temperature affects both the electrochemical responses. A number of factors are invoked to account for the variation of electrochemical behavior of the heat-treated complex. One of these is the structural change in the material during the thermal treatment. Indeed, the catalysts heated up to 270 °C yield identical responses arising from the Co^{3+}/Co^{2+} couple. The gradual decrease in magnitude of the current peaks with further heat treatment up to 670 °C is consistent with the decrease in concentration of cobalt ions on the electrode surface. For the electrodes heated to 800 °C, the reversible cathodic-anodic peak disappears, confirming the transformation of metal ions to other compounds, which agrees well with the structural analysis results. The second cathodic response also exhibits a correlation between the potential and the heating temperature, which is affected by decomposition of the adsorbed complex. This peak, less pronounced for the specimen treated in the interval 270–670 °C, increases in magnitude and shifts to more positive potentials, suggesting that heating provides a distinct catalytic effect on the oxygen reduction. The E_R response of both carbon supports to the pH increases immediately after the complex is absorbed, but then falls if the carbons are heated to 670 °C. For these specimens, the slow kinetics of peroxide decomposition is observed. The increase in oxygen overpotential and drop in the catalytic activity observed at 670 °C is presumably consistent with the regulation of the structure of the material occurring after the decomposition and release of the ligands.

The important revelation from the behavior observed is the more significant increase in the catalytic current of the specimen treated at 800 °C. The slope of dE_R/dpH increases when the temperature is raised to 800 °C, at which point, according to the thermal and IR experiments, the above-mentioned processes have been already completed. The measured values of –0.054 to –0.056 mV/pH unit of dE_R/dpH coincide well with the value of –0.059 mV/pH unit [25, 26, 27] for the reaction equilibrium O_2/OH^- estimated for the four-electron reaction of oxygen reduction through the catalytic decomposition of hydrogen peroxide. The rate of catalyzed peroxide decomposition is greater for these specimens, and the decomposition reaches 90–100%, suggesting these specimens to be excellent catalysts for these reactions in the whole pH range studied.

The voltammetric data reveal two features of the electrochemical behavior of the $(BPh)_2$[Fe(Nx)$_3$] complex. The inner-sphere iron ion remains essentially intact and does not show any cyclic voltammetric response. From the analysis of the E_R-pH diagrams and from the peroxide decomposition test, the modification of the carbon support by the $(BPh)_2$[Fe(Nx)$_3$] complex suppresses the catalytic activity of the carbon support.

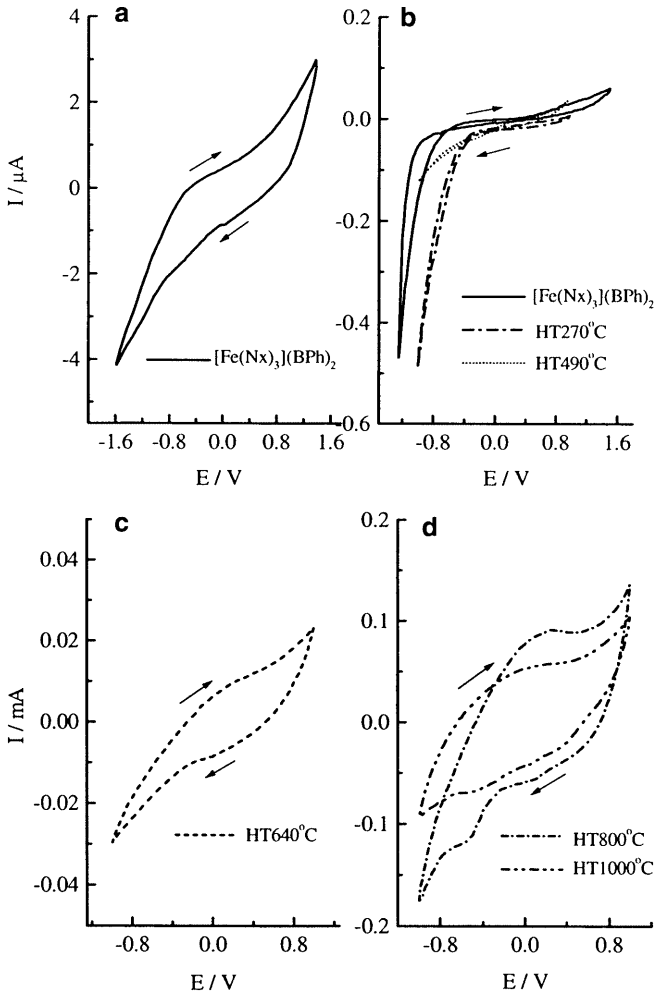

Fig. 10 Cyclic voltammograms recorded at the SCN carbon electrode for the dissolved $(BPh)_2[Fe(Nx)_3]$ complex (**a**) and the complex before and after heat treatment at different temperatures (**b–d**). Supporting electrolyte: **a** acetonitrile; **b–d** 0.15 mol dm^{-3} NaCl; scan rate: 20 mV s^{-1}; oxygen atmosphere

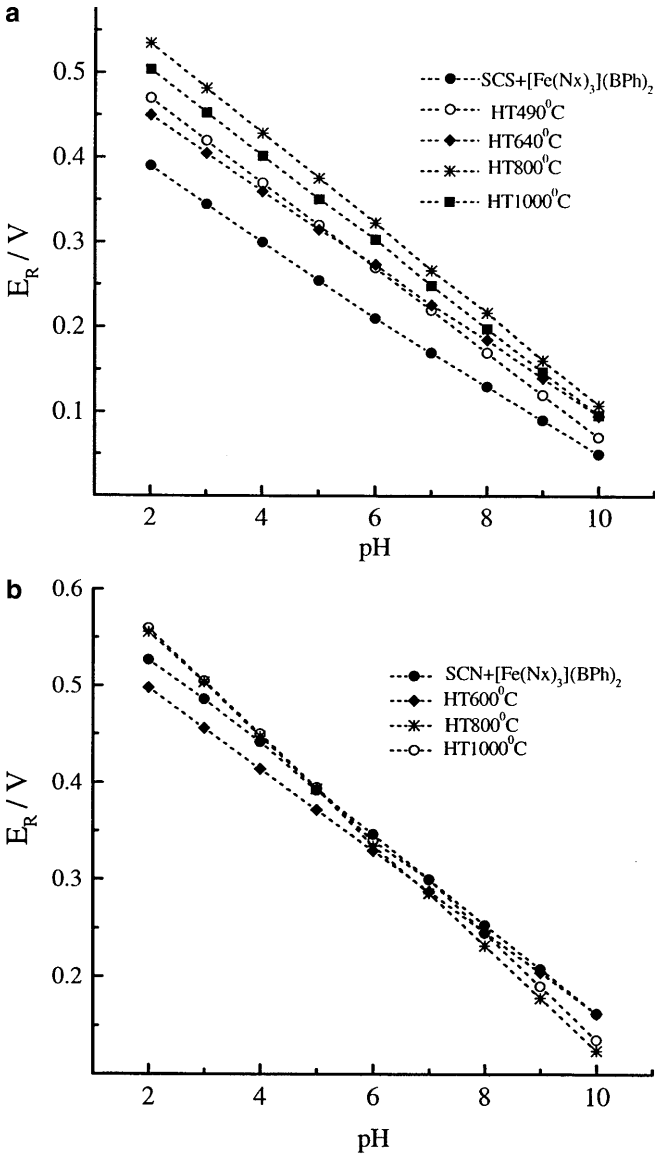

Fig. 11 The steady potential of the electrode, E_R, as a function of the pH for the **a** SCS- and **b** SCN-supported $(BPh)_2[Fe(Nx)_3]$ complex after various heat treatments. Supporting electrolyte: 0.15 mol dm^{-3} NaCl; oxygen atmosphere

Unlike the case of the $K_3[Co(Dmg)_3]$ complex, such a different behavior is likely to arise from the adsorption of catalytically inactive iron containing the complex on the carbon surface, which causes changes in the concentration of surface-active centers responsible for the oxygen reduction. On the other hand, similar to the $K_3[Co(Dmg)_3]$ complex, the $(BPh)_2[Fe(Nx)_3]$ complex treated at the higher temperatures also reveals high catalytic activity for peroxide decomposition and oxygen reduction. The catalytic activity was detected for the specimens treated at 800–1000 °C.

Interestingly, in view of the above discussion, the carbon-supported complexes heat treated to 800 °C are capable of oxygen reduction at more positive potentials and without forming a significant amount of hydrogen peroxide, owing to its entire decomposition at the electrode. Thus, the direct four-electron reduction of oxygen to water seems to proceed at these electrodes.

The effect of the adsorbed complex on the behavior of the carbon support can be explained in the following way. Since before decomposition the interaction between the complex and the carbon support occurs through the outer fringe, the activity of the prepared material depends mainly on the activity of the complex. Thus, while adsorbed, the electrochemically stable $(BPh)_2[Fe(Nx)_3]$ complex produces no effect on the carbon support, whereas the catalytically active $K_3[Co(Dmg)_3]$ complex improves substantially the catalytic properties of the carbon support. Additionally, the oxygen reduction activity correlates with the $M^{II} \rightleftharpoons M^{III}$ redox potential of the central metal ion: the iron ion, having very low redox potential, is a poor catalyst for the oxygen reduction, while much better performance is observed for the cobalt ion, which has intermediate redox potential and can reversibly bind oxygen. Moreover, being surrounded

Table 4 The variation in half-wave potential and hydrogen peroxide decomposition among the catalysts employed

Catalyst	$E_{1/2}$ (V)[a]	H_2O_2 decomposition (%)[b]	Specific rate of H_2O_2 decomposition (mol s^{-1} g^{-1})[c]
SCS + $(BPh)_2[Fe(Nx)_3]$	–	14.1	0.3
SCS + $(BPh)_2[Fe(Nx)_3]$ (HT 640 °C)	–0.65	31.6	0.9
SCS + $(BPh)_2[Fe(Nx)_3]$ (HT 800 °C)	–0.08	92.3	6.7
SCS + $(BPh)_2[Fe(Nx)_3]$ (HT 1000 °C)	–0.01	87.9	4.2
SCN + $(BPh)_2[Fe(Nx)_3]$	–	13.3	0.6
SCN + $(BPh)_2[Fe(Nx)_3]$ (HT 640 °C)	–	20.6	0.7
SCN + $(BPh)_2[Fe(Nx)_3]$ (HT 800 °C)	–0.09	97.1	7.5
SCN + $(BPh)_2[Fe(Nx)_3]$ (HT 1000 °C)	–0.03	99.2	5.4

[a]The potential at which the current of the second cathodic peak reaches one-half the limiting value
[b]Measured after 2 h of contact with the fluidized-bed layer of the catalyst
[c]Calculated for the first 30 min of the reaction

by the ligands, the cobalt ion does not lose its catalytic activity and remains active over the whole pH range.

At the higher temperatures, another part of the complex also begins to react, and the catalytic activity begins to depend on the surface changes which took place during the thermal treatment. Considering the results of the thermal and electrochemical experiments along with those of the structure investigations, the improved oxygen reduction characteristics may be due to the formation of active surface complexes of isolated metal sites in the environment, presumably surrounded by the thermally modified ligands. These surface complexes are probably derived from the reaction between the ligands of the complex and radicals at the carbon surface generated during the decomposition of the surface groups, which can improve in stability with the increase in the heating temperature, as has also been reported for iron porphyrin compounds [11, 14]. The decrease in catalytic activity of the specimens treated at about 670 °C is consistent with the formation of intermediate compounds between the carbon surface and the products of complex destruction, leading to blocking of the surface-active sites responsible for oxygen reduction. The decrease in the activity of the specimens treated at above 800 °C can be explained as being due to the destruction of these reactive surface complexes.

Conclusions

The electrochemical behavior and catalytic activity of macrobicyclic complexes of cobalt and iron and carbon-supported complexes in oxygen reduction in aqueous solutions were found to depend strikingly upon the structure of the complex and can be substantially improved by heat treatment in an argon atmosphere.

The $K_3[Co(Dmg)_3]$ complex was proved to have good adsorption ability and a highly stable performance in the redox and catalytic reactions, whereas the $(BPh)_2[Fe(Nx)_3]$ complex appeared to be catalytically inactive.

The heat-treated catalysts become capable of reducing the oxygen overpotential. The reaction proceeds at substantially more positive potentials than those estimated for the carbon-supported complex before the heat treatment. This effect was found to be more significant for the SCS carbon support. The optimal heating temperature for preparing the most effective catalyst was estimated to be 800–1000 °C.

Since there is now evidence for the effective performance of the modified carbon electrodes as catalysts for the electroreduction of molecular oxygen, it can be envisaged that carbon materials developed along these lines have the potential to become relatively inexpensive oxygen electrodes for energy conversion/storage systems or sensors.

Acknowledgements This research was supported by the Japan Science and Technology Corporation.

References

1. Tarasevich MR, Radyushkina KA (1981) Prog Surf Membr Sci 14:175
2. Shidehara K, Anson FC (1982) J Phys Chem 86:2776
3. Liu H, Abalmuhdi I, Chang CK, Anson FC (1985) J Phys Chem 89:665
4. Liu HY, Weaver MJ, Wang C-B, Chang CK (1983) J Electroanal Chem 145:439
5. Collman JP, Densevich P, Konai Y, Marrocco M, Koval C, Anson FC (1980) J Am Chem Soc 102:6027
6. Durand R, Anson FC (1982) J Electroanal Chem 132:107
7. Zagal J, Bindra P, Yeager Y (1980) J Electrochem Soc 127:1506
8. Holze R (1991) Electrochim Acta 36:999
9. Kuwana T, Fujihara M, Sunakawa K, Osa T (1978) Electroanal Chem 88:299
10. Wan G-X, Shigehara K, Tsuchida E, Anson F (1984) J Electroanal Chem 179:236
11. Van Veer JAR, Van Baar JF, Kroese KJ (1981) J Chem Soc Faraday Trans 1 77:2827
12. Van Veer JAR, Visser C (1979) Electrochim Acta 24:921
13. Janke H, Schönborn M, Zimmerman G (1976) Chem Forsch 61:133
14. Bagotzky VS, Tarasevich MR, Radyushkina KA, Levina OA, Andrusyova SI (1977/78) J Power Sources 2:233
15. Wiesenser K, Fuhrmann A (1980) Z Phys Chem (Leipzig) 261:411
16. Herl AJ, Sargeson AM, Harrowfield JM (1982) Australia Patent 525,243

17. Houlding V, Geiger T, Kölle U, Grätzel M (1982) J Chem Soc Chem Commun 681
18. Kostromina NA, Voloshin YaZ, Nazarenko AYu (1992) Clathrochelates: synthesis, structure, properties. Naukova Dumka, Kiev
19. Tymonov AM, Balashev KN, Shagusultanova GA, Fateev VN, Pakhomov VP, Chekmarev PM (1987) Elektrokhimiya 13:1061
20. Boston DR, Rose NJ (1968) J Am Chem Soc 90:6859
21. Johnson JN, Rose JN (1982) Inorg Synth 21:112
22. Basova YuV (2000) Electrochemistry 68:639
23. Bettelheim A, Chan RJH, Kuwana T (1980) J Electroanal Chem 110:93
24. Brown AP, Anson FC (1977) Anal Chem 49:1589
25. Kinoshita K (1988) Carbon, electrochemical and physicochemical properties. Wiley-Interscience, New York
26. Tarasevich MR (1984) Electrochemistry of carbon materials Nauka, Moscow
27. Bockris JO'M, Reddy AKN (1973) Modern electrochemistry. Plenum, New York